Active and Reactive Power Control of a DFIG For Variable Speed Wind Energy Conversion

F. Mazouz[1*], S. Belkacem[1], Y. Harbouche[1], R. Abdessemed[1] and S. Ouchen[2]

***Abstract* — In this paper, we propose a vector control of a doubly fed induction generator (DFIG) for variable speed wind power generation. The model is developed based on the dual powered generator for the control of the active and reactive powers. Several studies are carried out to test their operation under different wind conditions. The results have shown good performances of the wind energy converter system operate under wind variations with indirect vector control strategies.**

***Keywords* — Wind, Turbine, Doubly Fed Induction Generator, DFIG, Direct Vector control, Indirect Vector control, Active powers, Reactive powers.**

I. INTRODUCTION

To coincide with worsening concerns about depletion of fuel reserves worldwide, as well as carbon dioxide emissions, has found renewable sources of energy more attention [1], In recent years, the field of wind energy has grown rapidly, For the European Union, wind energy production accounted for 10.5% of the electricity generation mix in 2011, while in 2000 it was 2.2%, These percentages show that wind power has become a particularly important source of electricity generation in many countries and is expected to provide more electric power in the future. [2].

Most of turbine generator technology installed in power systems today is the doubly fed induction generator (DFIG) [1], [3]. The DFIM is a variable speed machine, but can deliver power with a constant voltage and frequency, as its rotational speed of the rotor fluctuates. When a bidirectional converter is installed, the range of rotor speed can be prolonged beyond the synchronous speed; consequently, the electrical power is produced from the stator and rotor [3]. The DFIG offers more advantages: better efficiency, variable speed to obtain the maximum power extracted from the wind, adaptable power factor, ability to control reactive power and less converter [3]. The large penetration of wind power generation in the grid will affect the system's stability, particularly the voltage stability; consequently, the effect of the DFIG on system stability has become the subject of intense research in recent years. [3].

The method of controlling the DFIG organized in this article is given as follows:

- Supply a synthesis of the fundamental principles and current schemes of the turbine and DFIG
- Provides the details of a control overall system
- Gives the analysis, the results, and concludes the main findings of the research.

II. MODEL DESCRIPTION

A typical wind turbine is comprised of a generator, a gearbox, a converter and the transformer [4]. The converter connecting the rotor of generator and a source of three phase power [5]. A schematic diagram of a typical conversion system is shown in Figure 1:

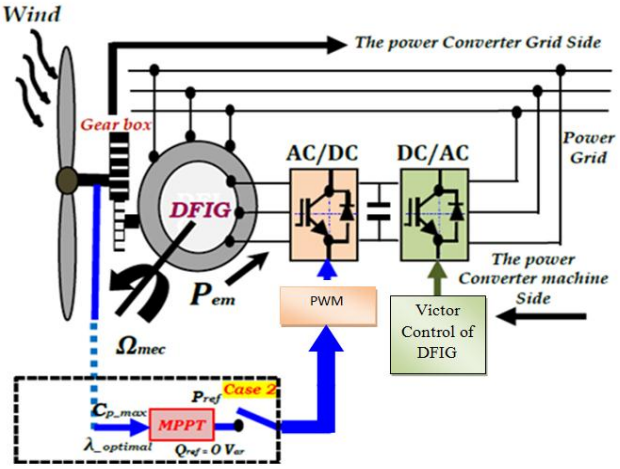

Figure 1. Schematic diagram of a typical conversion system in a wind turbine

In the case where the wind speed is low, the inverter receives power from the grid and sets the magnetization of the stator [4].

III. TURBINE MODELE

By applying the theory of momentum and Bernoulli's one can determine the incident power due to wind, which is given by the following equation, [6]:

$$P_v = \frac{1}{2}.\rho.S.v^3 \qquad (1)$$

*Mazouz Farida, e-mail: fari_maz@yahoo.fr
[1]Electrical Engineering Laboratory LEB, University of Batna2, Algeria.
[2]Electrical Engineering Laboratory of Biskra LGEB, University of Mohammed Khider, Biskra, Algeria Amor Bourek

with:

S: is the area of the wind wheel (m^2);

ρ: the air density (ρ=1.225 kg /m^3 atmospheric pressure 15°C);

v: wind speed (m/s);

The mechanical power captured by the turbine from the wind is given by the following expression: [7]:

$$P_{aer} = C_p.P_v = \frac{1}{2} C_p(\beta,\lambda).\rho.S.v^3 \quad (2)$$

Where $C_p(\beta,\lambda)$ is the power coefficient of the turbine, ratio λ is the tip speed ratio and β is the pitch angle. The tip speed ratio is given by the following equation: [6]:

$$\lambda = \frac{R.\ \Omega_{\text{turbine}}}{v} \quad (3)$$

Where R is the turbine radius,Ω_{turbine} the speed of the turbine

Maximum value of Cp is fixed by Betz constant, as follows [6], [7], [8]:

$$C_p(\beta,\lambda) = \frac{Pm}{Pwind} = \frac{16}{27} = 0.59$$

Can be modeled with a power coefficient equation that depends on the speed ratio λ and the orientation angle β of the blades. For example, expression of a wind turbine power coefficient of 1.5 MW is approximated by the equation [9]:

$$C_p(\lambda,\beta) = (0.5 - 0.0167.(\beta-2)).\sin\left[\frac{\pi.(\lambda+0.1)}{18.5-0.3.(\beta-2)}\right] - 0.00184.(\lambda-3).(\beta-2) \quad (4)$$

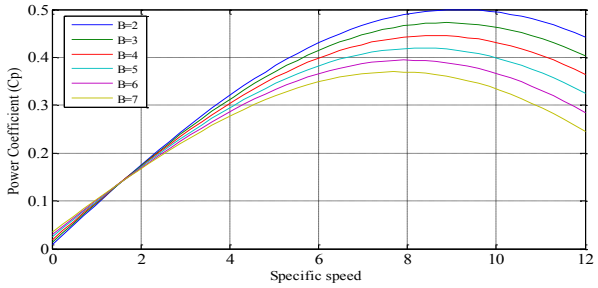

Figure 2. Evolution of the power coefficient with the variation of the relative speed of the turbine.

The characteristic of the speed relative to the power factor for the different values of λ is shown in Figure 2. This gives a maximum power coefficient of 0.5 for a speed ratio λ which is 9.2 (λ opt) [9].

The aerodynamic torque on the slow axis can be expressed by equation 5:

$$C_{aer} = \frac{P_{aer}}{\Omega_{\text{turbine}}} = C_p(\beta,\lambda)\frac{1}{2}\rho S v^3 \frac{1}{\Omega_{\text{turbine}}} \quad (5)$$

The total inertia J is made up of the turbine inertia brought on the fast axis and inertia generator J_g.

$$J = \frac{J_{turbine}}{G^2} + J_g \quad (6)$$

with :

J_{turbine}: inertia of the turbine

J_g: inertia of the generator.

To determine the evolution of the mechanical speed from the total torque C_{mec} applied to the rotor of DFIG, the basic equation is applied to the dynamic:

$$C_g - C_{em} = J.\frac{d\Omega_{mec}}{dt} + f.\Omega_{mec} \quad (7)$$

$\Omega_{méc}$: mechanical speed of DFIG.

C_{em}: electromagnetic torque.

f: coefficient of friction.

IV. EXTRACTION TECHNIQUES OF HIGH POWER

In this part, we present various strategies to control the electromagnetic torque (and indirectly the electromagnetic power converted) to adjust the mechanical speed to maximize the generated electric power.

- The servo control without mechanical speed;
- The servo control with mechanical speed;

A. Maximizing power without speed control

If the wind speed is measured and the mechanical characteristics of the wind turbine are known, it is possible to derive real-time optimal mechanical power that can be generated with the monitoring of maximum power point tracking (MPPT). The optimal mechanical power can be expressed as [10]

$$C_{em_{ref}} = \frac{1}{2}\frac{C_{pmax}}{\lambda_{opt}^3}.\rho.\pi.R^5.\frac{\Omega_{mec}^2}{G^3} \quad (8)$$

Where λ_{opt} the optimum tip speed ratio

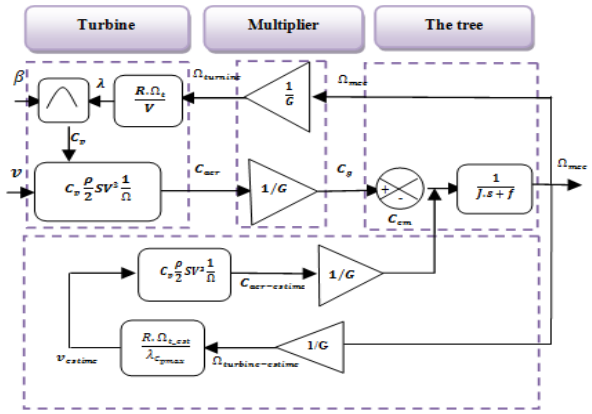

Figure 3. Block diagram of maximizing the power extracted without speed control.

From this equation, we can construct the block diagram of maximizing the power without speed control, shown in figure 3.

B. *Maximizing power with speed control*

In order to extract the maximum power of the incident wind, permanently must adjust the rotational speed of the turbine to the wind. The speed of DFIG is used as a reference value for a proportional-integral controller type (phase lead PI) as shown in the following figure:

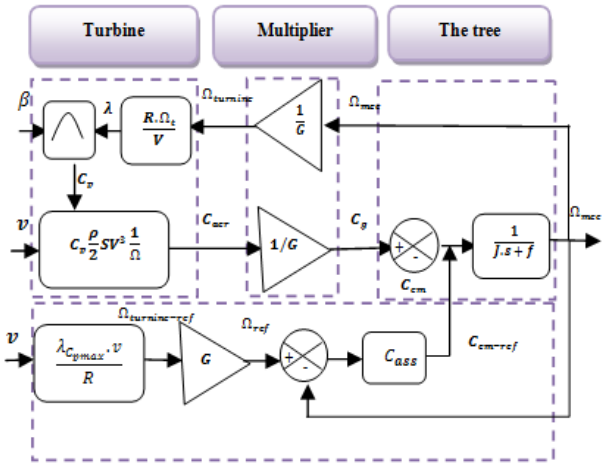

Figure 4. Block diagram of maximizing the power extracted with speed control.

This determines the control set point which is the electromagnetic torque that should be applied to the machine to run the generator at its optimal speed. The pair thus determined by the regulator is used as reference variable torque model of the turbine (Figure 4) pitch angle of the blades is changed (variation of the angle of incidence) to change the ratio between lift and drag. To extract the maximum power (and keep constant), adjusting the angle of the blades to the wind speed.

$$C_{em-ref} = C_{ass}.(\Omega_{ref} - \Omega_{mec}) \tag{9}$$

V. ACTIVE AND REACTIVE POWERS CONTROL OF THE DFIG

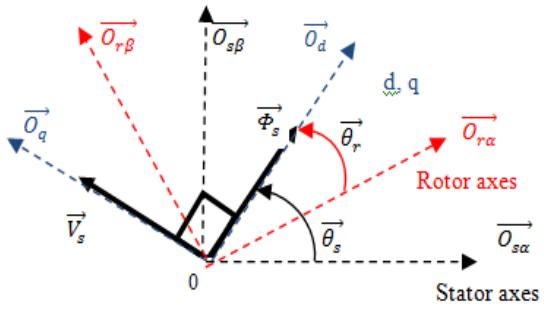

Figure 5. Voltage and stator flux Orientation..

For the vector control of this generator, it is necessary to choose a reference related to the rotating field. The cue Park would, therefore, synchronized with the stator flux [12], whose axis is aligned with the stator flux vector, as shown in figure 5.

A. *Modeling of the DFIG*

The dynamic equations of the DFIG in the reference d-q can be written as follows [12], [8].

The voltages equations are given by:

$$\begin{cases} V_{ds} = R_s I_{ds} + \dfrac{d\varphi_{ds}}{dt} - \omega_s \varphi_{qs} \\ V_{qs} = R_s I_{qs} + \omega_s \varphi_{ds} + \omega_s \varphi_{qs} \\ V_{dr} = R_r I_{dr} + \dfrac{d\varphi_{dr}}{dt} - (\omega_s - \omega)\varphi_{qr} \\ V_{qr} = R_r I_{qr} + \dfrac{d\varphi_{qr}}{dt} + (\omega_s - \omega)\varphi_{dr} \end{cases} \tag{10}$$

The flux equations are given by:

$$\begin{cases} \varphi_{ds} = L_s I_{ds} + M I_{dr} \\ \varphi_{qs} = L_s I_{qs} + M I_{qr} \\ \varphi_{dr} = L_r I_{dr} + M I_{dr} \\ \varphi_{qr} = L_r I_{qr} + M I_{qr} \end{cases} \tag{11}$$

The arrangement of the equations (10) and (11) gives the expression of the rotor voltages according to the rotor currents by:

$$\begin{aligned} V_{dr} &= R_r I_{dr} + \left(L_r - \frac{M^2}{L_s}\right)\frac{dI_{dr}}{dt} - g\omega_s\left(L_r - \frac{M^2}{L_s}\right) I_{qr} \\ V_{qr} &= R_r I_{qr} + \left(L_r - \frac{M^2}{L_s}\right)\frac{dI_{qr}}{dt} + g\omega_s\left(L_r - \frac{M^2}{L_s}\right) I_{dr} + g\frac{MV_s}{L_s} \end{aligned} \tag{12}$$

The torque equation is represented as follows:

$$C_{em} = p\frac{M}{L_s}(I_{qr}\varphi_{ds} - I_{dr}\varphi_{qs}) \tag{13}$$

The supplied active and reactive power is defined as follows:

$$\begin{cases} P_s = V_{ds} I_{ds} + V_{qs} I_{qs} \\ Q_s = V_{qs} I_{ds} - V_{ds} I_{qs} \end{cases} \tag{14}$$

Adopting the assumption of a negligible stator resistance Rs and the stator flux is constant and oriented along the axis, we deduce:

$$\varphi_{ds} = \varphi_s \quad \text{et} \quad \varphi_{qs} = 0$$

$$\begin{cases} V_{ds} = \dfrac{d\varphi_s}{dt} = 0 \\ V_{qs} = V_s = \omega_s \varphi_s \end{cases} \tag{15}$$

The stator active and reactive power can be expressed as the rotor currents as follows:

$$\begin{aligned} P_s &= -V_s \frac{M}{L_s} I_{qr} \\ Q_s &= \frac{V_s^2}{L_s \omega_s} - V_s \frac{M}{L_s} I_{dr} \end{aligned} \tag{16}$$

From the Presidents equations we can construct the scheme of DFIG illustrated in figure 6:

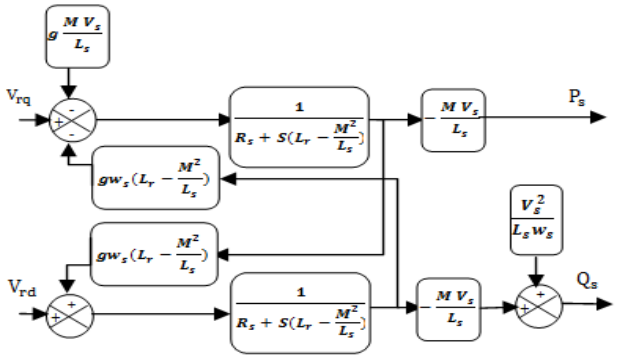

Figure 6. Simplified diagram of the DFIG

B. Direct Control of Active and Reactive Powers

In this method using two PI controllers; two control the machine, we will set up a control loop of each power (Ps and Qs) with an independent regulator while compensating the disturbance terms that are present in the block diagram in Figure 6. We neglect the terms of coupling between the two axes of control because of the low value of the slip. We obtain a vector control with a single controller per axis, shown in Figure 7, [12], [13].

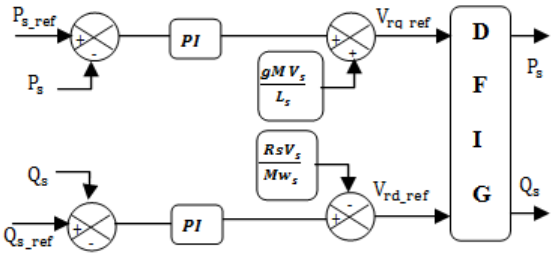

Figure 7. Block diagram of the direct control.

C. Indirect Control of Active and Reactive Power

1) Indirect control loops without the power:

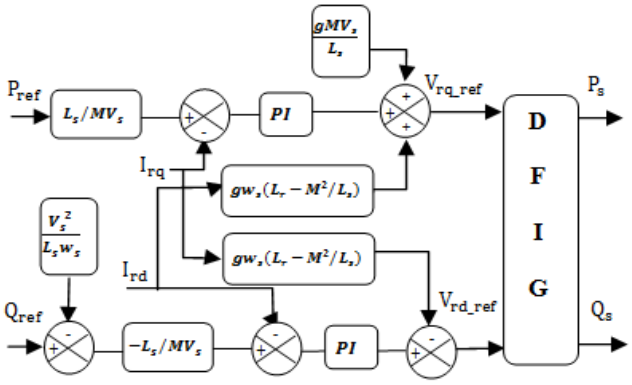

Figure 8. Block diagram of indirect control in open loop.

The rotor currents irq and ird, respectively images of the stator active and reactive power Ps and Qs, should continue their current references, [12].

2) Indirect control loops with the Powers:

To improve the previous control, we will incorporate additional control loop at the powers to eliminate the static error while preserving the system dynamics [13].

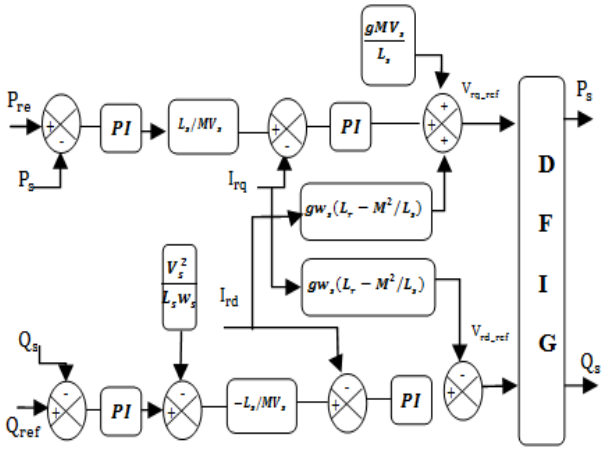

Figure 9. Block diagram of indirect control in closed loop.

VI. SIMULATION RESULTS

The direct active and reactive power control algorithm is simulated on the MATLAB/SIMULINK platform. In this section the simulation results are presented in order to highlight the robustness of the proposed algorithm. The system is subject to wind speed of 7.5 m / s.

The active power reference is given by the power supplied by the turbine is given by two constant values ranging between (1000 and 1500). Simulation results are shown in the following figures:

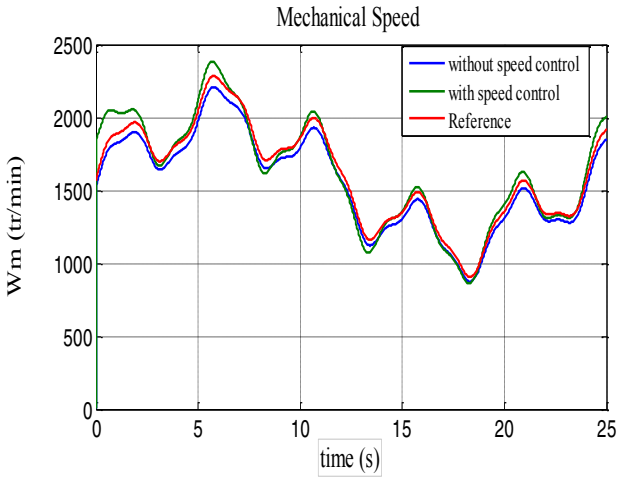

Figure 10. Mechanical speed Wm (tr/min).

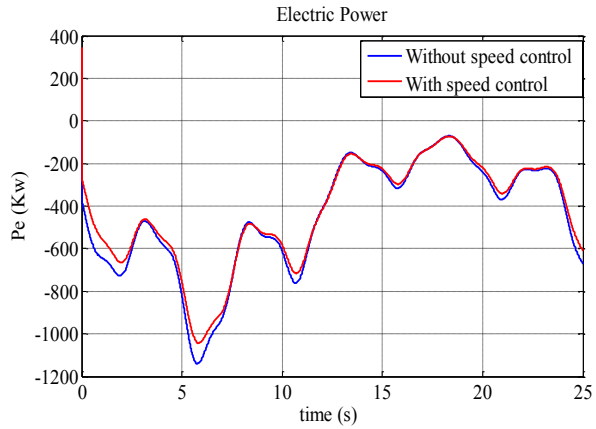

Figure 11. Power Pe (Watt).

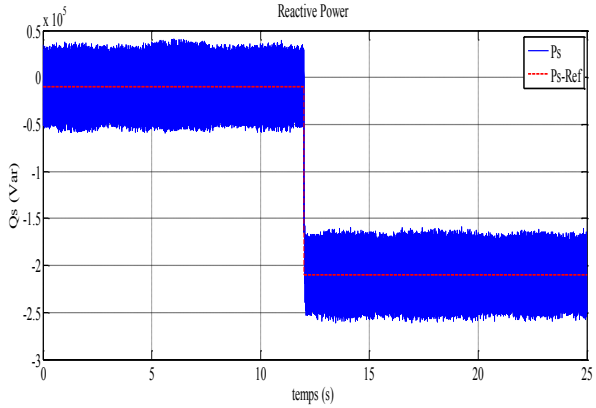

Figure 12. Reactive power Qs (Var)

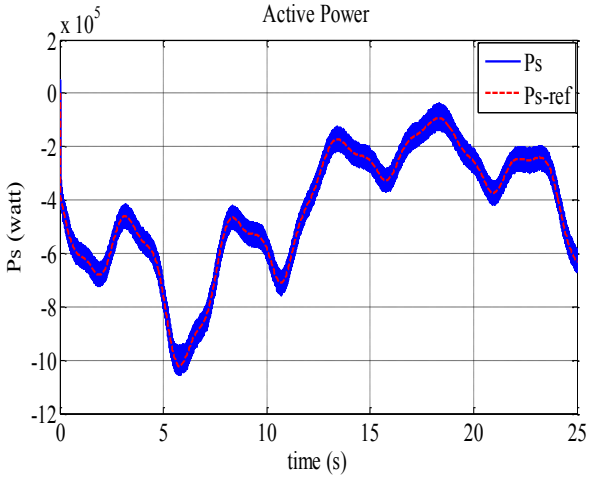

Figure 13. Active power Ps (Watt)

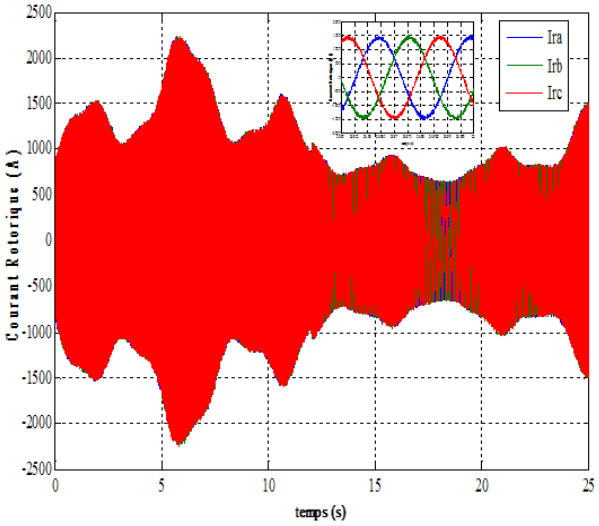

Figure 14. Rotor current Ir (A).

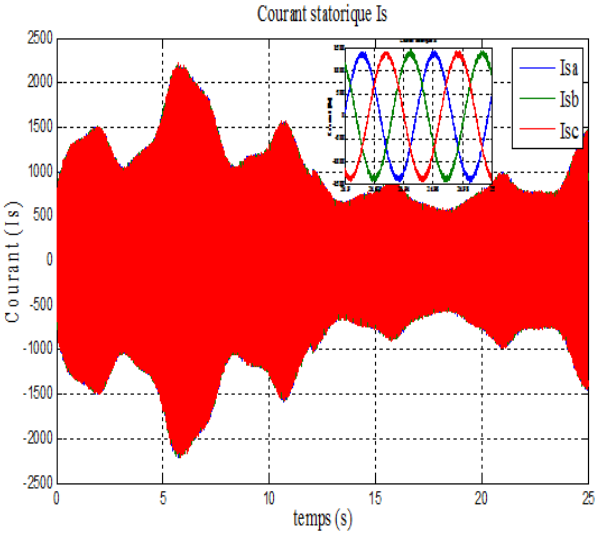

Figure 15. Stator current Is (A)

Figure 16.

To summarize these results with either the speed control strategy, Figure 10 and 11 show the mechanical speed and its reference and the electrical power obtained with the two types of control.

The simulation results corresponding to this control algorithm show that variation of the speed of the generator is adapted to the variation of the wind speed, the electromagnetic power into electrical power produced is very fluctuating.

The simulation results shown in Figures 12, 13, 14 and 15 shows the different curves obtained by controlling the active and reactive power generated in the stator of the DFIG. This command has to decouple the active power is reactive generator. The quadrature component of the rotor current iqr control the electromagnetic torque and the direct component

idr control reactive power exchanged between the stator and the network.

The technique of indirect closed loop control (power loop) is more efficient than direct control that has more disturbances between the two powers. Indirect control loops with and without powers have almost the same performance. However those without powers loop is faster because it uses four controllers.

VII. CONCLUSION

In this paper, an approach has been proposed to control the active and reactive power and improve the quality of the grid power using a WECS equipped by a DFIG.

Simulation results confirm the effectiveness and robustness of the proposed DPC strategy during various operating conditions and parameter variations.

VIII. PARAMETERS DE SUMULATION

TABLE I. TURBINE PARAMETERS

Balde radius, R	35.25
Number of blades	3
Gearbox ratio, G	90
Moment of inertia, J	1000 Kg.m^2
Viscous friction coefficient, f	0.0024 N.m.s^{-1}
Cut-in wind speed	4 m/s
Cut-out wind speed	25 m/s
Nominal wind speed, v	16 m/s

TABLE II. DFIG PARAMETERS

Rated power, Pn	1.5 MW
Stator rated voltage, Vs	398/690 V
Rates current, In	1900 A
Rated DC-link voltage U_{DC}	1200 V
Stator rated frequency, f	50 Hz
Stator inductance, Ls	0.0137 H
Rotor inductance, Lr	0.0136 H
Mutual inductance, M	0.0135 H
Stator resistance, Rs	0.012 Ω
Rotor resistance, Rr	0.021 Ω
Number of pair of poles, P	2

IX. REFERENCES

[1] M. Pichan, H. Rastegar, M. Monfared, «Two fuzzy-based direct power control strategies for doubly-fed induction generators in wind energy conversion systems », Science Direct, Energy, vol. 5, 2013, pp.154-162.

[2] F. Girbau-Llistuella, A. Sumper, F. Díaz-González, S Galceran-Arellano, «Flicker mitigation by reactive power control in wind farm with doubly fed induction generators», Science Direct, Electrical Power and Energy Systems, vol. 55, 2014, pp. 285–296.

[3] A. Arief, Z. Y. Dongb, M. B. Nappua, M. Gallagherc, «Under voltage load shedding in power systems with wind turbine-driven doubly fed induction generators», Science Direct, Electric Power Systems Research, vol. 96, 2013, pp. 91– 100.

[4] C. W. Zhang, T. Zhang, N. Chen, T. Jin, «Reliability modeling and analysis for a novel design of modular converter system of wind turbines», Science Direct, Reliability Engineering and System Safety , vol. 111, 2013, pp. 86–94.

[5] H. Mahmoudi, M. E. Ghamrasni, A. Lagrioui, B. Bossoufi, «backstepping adaptive control of DFIG generators for wind turbines variable-speed», Journal of Theoretical and Applied Information Technology, Vol. 81. N° 2. 20th November 2015, pp. 320-330.

[6] Gaillard A, Poure P, Saadate S, Machmoum M. Variable speed DFIG wind energy system for power generation and harmonic mitigation. Renewable Energy 2009.

[7] Mohsen R, Mostafa P. Transient performance improvement of wind turbines with doubly fed induction generators using nonlinear control strategy. IEEE Transactions on Energy Conversion June 2010.

[8] A. Tamaarat, A. Benakcha, «Performance of PI controller for control of active and reactive power in DFIG operating in a grid-connected variable speed wind energy conversion system», Front. Energy vol. 8, n°3, 2014, pp. 371–378.

[9] Kayikçi M, Milanovic J. Reactive power control strategies for DFIG-based plants. IEEE Transactions on Energy Conversion 2007.

[10] H. Amimeur, D. Aouzellag, R. Abdessemed, K. Ghedamsi, «Sliding mode control of a dual-stator induction generator for wind energy conversion systems», Electrical Power and Energy Systems vol. 42, 2012, pp. 60–70.

[11] Z. Gadouche , C. Belfedel, T. Allaoui, B. Belabbas, «Commande de Puissance Active et Réactive d'une MADA utilisée dans un système éolien», 3ème Séminaire International sur les Energies Nouvelles et Renouvelables, Ghardaïa – Algérie Octobre 13-14, 2014.

[12] Forchetti D, Garcia G, Valla MI. Vector control strategy for a doubly-fed standalone induction generator. In: IEEE 2002 28th annual conference of the industrial electronics society; 2002.

[13] A. Petersson, Analysis, modeling and control of doubly-fed induction generators for wind turbines, Ph.D. Thesis, Chalmers University of Technology, Goteborg, Sweden, 2005.